

## Screening of a Fixed Charge in Bismuth Metal\*†

D. H. BROWNELL, JR.,‡ AND E. H. HYGH

*Department of Physics, University of Utah, Salt Lake City, Utah*

(Received 20 July 1967)

The screening-charge density and the potential matrix elements of a fixed charge in bismuth are calculated using a density-matrix approach. Numerical values of the charge density in the three principal crystal directions are obtained using the band parameters of Smith, Baraff, and Rowell. The resulting charge-density oscillations are interpreted on the basis of the band structure of bismuth.

## I. INTRODUCTION

THE present study was undertaken in order to explain from first principles the Alfvén-wave relaxation-time data of McLachlan.<sup>1</sup> Neither these data nor, for example, the dc resistivity data of Zitter<sup>2</sup> can be explained on the assumption of (unequal) isotropic relaxation times for the electron and hole portions of the Fermi surface of bismuth. We have thus undertaken to treat the scattering of electrons and holes by ionized impurities; even in the purest obtainable bismuth samples, impurity scattering seems to be dominant at temperatures near and below 4.2°K.

This paper will treat the screening of an ionized impurity using the self-consistent field (SCF) approach due to Ehrenreich and Cohen<sup>3</sup>; for the isotropic electron gas, this method is known to yield results equivalent to those obtained from the random-phase approximation (RPA).<sup>4</sup> A subsequent paper<sup>5</sup> will apply these results to the damping of Alfvén waves, using the Boltzmann-equation formulation.

The calculation of the screened potential and the induced charge density due to a fixed-point charge in the isotropic electron gas at absolute zero has been carried out by Langer and Vosko<sup>6</sup> using two diagrammatic approaches, one due to Hubbard<sup>7</sup> and the other to Gell-Mann and Brueckner.<sup>8</sup> The latter approach gives results identical to those of the SCF and RPA. In particular, one obtains, for the induced charge density at large distances from the impurity, the char-

acteristic "Friedel oscillations":

$$n_1(r) \approx Cr^{-3} \cos 2k_F r, \quad (1)$$

where  $k_F$  is the Fermi wave number and  $C$  is a constant. A similar result has been obtained by Friedel<sup>9</sup> using an independent-particle approach. We will find the asymptotic limit of the charge density in bismuth to be the sum of terms of the form of Eq. (1), but with a somewhat anisotropic character, as one expects from the rhombohedral symmetry of bismuth.

In recent years many experiments have been carried out with the aim of obtaining a detailed knowledge of the structure of the hole and electron conduction bands in bismuth. We will not go into great detail about the relative merits of these experiments and the reliability of the conclusions drawn from them. We merely mention that it appears fairly certain that the Fermi surface consists of three electron ellipsoids with band minima located at points  $L$  in the zone (see Fig. 1), and a hole ellipsoid at point  $T$ . In any case, for the purposes of this paper the location of the band minima is immaterial, except that we assume the minima are separated in  $\mathbf{k}$  space by distances large compared to the maximum dimensions of any of the carrier ellipsoids. We also mention the very close agreement between the band parameters obtained by Smith, Baraff, and Rowell (SBR)<sup>10</sup> from magnetoresistance measurements, the magnetoreflexion data of Maltz and Dresselhaus,<sup>11</sup> and the magnetoacoustic data of Sawada and Burstein.<sup>12</sup>

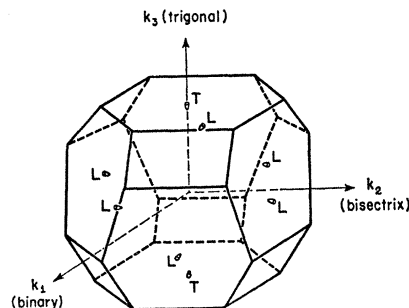


FIG. 1. The Brillouin zone of bismuth. The electron half-ellipsoids at  $L$  and the hole half-ellipsoids at  $T$  project into the zone.

\* Supported in part by the U. S. Air Force Office of Scientific Research, Grant No. AF-AFOSR-901-65 and in part by the National Science Foundation.

† Based on part of a thesis submitted by D. H. Brownell, Jr. in partial fulfillment of the requirements for the Doctor of Philosophy degree at the University of Utah, 1967.

‡ National Science Foundation Graduate Trainee. Present address: Department of Physics and Astronomy, Louisiana State University, Baton Rouge, Louisiana.

<sup>1</sup> D. S. McLachlan, *Phys. Rev.* **147**, 368 (1966).

<sup>2</sup> R. N. Zitter, *Phys. Rev.* **127**, 1471 (1962).

<sup>3</sup> H. Ehrenreich and M. H. Cohen, *Phys. Rev.* **115**, 786 (1959).

<sup>4</sup> D. Pines, *Elementary Excitations in Solids* (W. A. Benjamin, Inc., New York, 1963).

<sup>5</sup> D. H. Brownell, Jr. and E. H. Hygh, *Phys. Rev.* **164**, 916 (1967).

<sup>6</sup> J. S. Langer and S. H. Vosko, *J. Phys. Chem. Solids* **12**, 196 (1959).

<sup>7</sup> J. Hubbard, *Proc. Roy. Soc. (London)* **A240**, 539 (1957); **A243**, 336 (1957); **A244**, 199 (1958).

<sup>8</sup> M. Gell-Mann and K. Brueckner, *Phys. Rev.* **106**, 364 (1957).

<sup>9</sup> J. Friedel, *Advan. Phys.* **3**, 446 (1954).

<sup>10</sup> G. E. Smith, G. A. Baraff, and J. M. Rowell, *Phys. Rev.* **135**, A1118 (1964).

<sup>11</sup> M. S. Maltz and M. S. Dresselhaus (unpublished).

<sup>12</sup> Y. Sawada and E. Burstein, *Phys. Rev.* **150**, 456 (1966).

The results of these three experiments are successfully interpreted on the basis of the so-called two-band model proposed by Lax<sup>13</sup>; therefore, we will use this model for our calculations.

In the two-band model, the electron energy  $\epsilon$  in the conduction band (measured from the band minimum) is given by

$$\epsilon(1 + \epsilon/\epsilon_G) = \frac{1}{2}\hbar^2\mathbf{k} \cdot \boldsymbol{\alpha}^{(i)} \cdot \mathbf{k}, \quad (2)$$

where  $\epsilon_G$  is the gap energy (i.e., the energy difference between the band extrema of the conduction and valence bands),  $\hbar\mathbf{k}$  the crystal momentum measured from the band minimum, and  $\boldsymbol{\alpha}^{(i)}$  the inverse mass tensor of ellipsoid  $i$  at the bottom of the conduction band. In the system of axes 1=binary, 2=bisectrix, 3=trigonal,  $\boldsymbol{\alpha}$  has the form

$$\boldsymbol{\alpha}^{(A)} = \begin{pmatrix} \alpha_1 & 0 & 0 \\ 0 & \alpha_2 & \alpha_4 \\ 0 & \alpha_4 & \alpha_3 \end{pmatrix} \quad (3)$$

for one ellipsoid (which we call ellipsoid A); the  $\boldsymbol{\alpha}^{(i)}$  for the two other electron ellipsoids (B and C) are given by rotating the tensor in Eq. (3) by  $\pm 120^\circ$ , respectively, about the trigonal axis. The hole ellipsoid is assumed parabolic, with hole energy given by

$$\epsilon = \frac{1}{2}\hbar^2\mathbf{k} \cdot \boldsymbol{\alpha}^{(H)} \cdot \mathbf{k}, \quad (4)$$

where  $\epsilon$  and  $\hbar\mathbf{k}$  are measured from the hole-band minimum. The form of  $\boldsymbol{\alpha}^{(H)}$  is, by crystal symmetry,

$$\boldsymbol{\alpha}^{(H)} = \begin{pmatrix} \alpha_{H1} & 0 & 0 \\ 0 & \alpha_{H1} & 0 \\ 0 & 0 & \alpha_{H3} \end{pmatrix}. \quad (5)$$

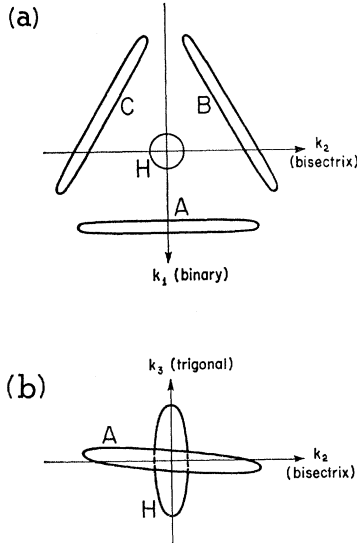


FIG. 2. Connected electron and hole ellipsoids in bismuth, looking (a) along the trigonal axis, and (b) along the binary axis. Distances between band minima are not drawn to scale.

<sup>13</sup> M. Lax, Bull. Am. Phys. Soc. 5, 167 (1960).

The band parameters obtained by SBR are given in Table I. The hole energy  $\epsilon_H$  plays the role of the Fermi energy for the holes.

To calculate the impurity screening and transport properties of bismuth, we need to know only the band parameters of Table I, and in addition, the lattice dielectric tensor  $\boldsymbol{\epsilon}_l$ . If the SBR parameters are assumed, then a value of  $\epsilon_l = 100$  is consistent with the infrared absorption data of Boyle and Brailsford.<sup>14</sup> We shall use this value, which is current in the literature, and in the numerical calculations we shall assume that the tensor  $\boldsymbol{\epsilon}_l$  is isotropic. Thus our calculation uses nine independent parameters, all of which are taken from experimental data.

## II. SCREENING OF AN IONIZED IMPURITY

We consider the electrons in bismuth at  $T=0$ . To begin with, we take the electron and hole half-ellipsoids shown in the reduced zone scheme in Fig. 1, and connect the band extrema through appropriate reciprocal lattice translations. The result is shown in Fig. 2. In the spirit of the SCF approach, we now consider a system of electrons in states  $|\mathbf{k}, l\rangle = u_{\mathbf{k}, l} e^{i\mathbf{k} \cdot \mathbf{x}}$ , which are eigenfunctions of a Hamiltonian  $H_0$  with energy  $\epsilon_{0\mathbf{k}, l}$ , and are normalized to unit volume. Here  $u_{\mathbf{k}, l}$  is a Pauli spinor,  $\mathbf{k}$  is the electron wave vector, and  $l$  is the band index. For generality, we assume the electrons are in a medium with lattice dielectric tensor  $\boldsymbol{\epsilon}_l$ . In this section,  $\mathbf{k}$  includes the spin index.

We consider next the detailed nature of the single-electron density matrix  $\rho$ . If we add to  $H_0$  a perturbation potential

$$H_1(\mathbf{x}, t) = V(\mathbf{x})e^{(-i\omega + s/\hbar)t}, \quad (6)$$

and expand the density matrix in the form

$$\rho = \rho_0 + \rho_1 e^{(-i\omega + s/\hbar)t}, \quad (7)$$

where  $\rho_0$  is the unperturbed density matrix, then the equation of motion for  $\rho$ , namely

$$i\hbar\dot{\rho} = [H, \rho], \quad (8)$$

yields, on dropping the second-order term  $[H_1(\mathbf{x}, t), \rho_1]$ , the expression

$$(\hbar\omega + is)\rho_1 = [H_0, \rho_1] + [V, \rho_0]. \quad (9)$$

TABLE I. The bismuth band parameters of Smith, Baraff, and Rowell.<sup>a</sup> The electron  $\alpha_i$  are at the bottom of the band. The first eight parameters listed are independent; the other two may be derived from them.

$\alpha_1 = 885.0m_0^{-1}$	$\alpha_{H1} = 15.63m_0^{-1}$
$\alpha_2 = 5.742m_0^{-1}$	$\alpha_{H3} = 1.449m_0^{-1}$
$\alpha_3 = 337.0m_0^{-1}$	$\epsilon_G = 15.3 \text{ meV}$
$\alpha_4 = 25.27m_0^{-1}$	$\epsilon_F = 27.6 \text{ meV}$
$\epsilon_H = 10.9 \text{ meV}$	$n = 2.75 \times 10^{17} \text{ cm}^{-3}$

<sup>a</sup> See Ref. 10.

<sup>14</sup> W. S. Boyle and A. D. Brailsford, Phys. Rev. 120, 1943 (1960).

Here  $s$  is the adiabatic "switching-on" parameter; in each expression the limit  $s \rightarrow +0$  is assumed. Using the fact that

$$\rho_0|\mathbf{k}, l\rangle = f_0(\epsilon_{0\mathbf{k}, l})|\mathbf{k}, l\rangle, \quad (10)$$

where  $f_0$  is the distribution function, and

$$H_0|\mathbf{k}, l\rangle = \epsilon_{0\mathbf{k}, l}|\mathbf{k}, l\rangle, \quad (11)$$

we can take matrix elements of both sides of Eq. (9):

$$\begin{aligned} (\hbar\omega + is)\langle \mathbf{k}, l | \rho_1 | \mathbf{k} + \mathbf{q}, l' \rangle \\ = (\epsilon_{0\mathbf{k}, l} - \epsilon_{0\mathbf{k} + \mathbf{q}, l'}) \langle \mathbf{k}, l | \rho_1 | \mathbf{k} + \mathbf{q}, l' \rangle \\ + [f_0(\epsilon_{0\mathbf{k} + \mathbf{q}, l'}) - f_0(\epsilon_{0\mathbf{k}, l})] \langle \mathbf{k}, l | V | \mathbf{k} + \mathbf{q}, l' \rangle. \end{aligned} \quad (12)$$

Thus,

$$\begin{aligned} \langle \mathbf{k}, l | \rho_1 | \mathbf{k} + \mathbf{q}, l' \rangle \\ = \frac{f_0(\epsilon_{0\mathbf{k} + \mathbf{q}, l'}) - f_0(\epsilon_{0\mathbf{k}, l})}{\epsilon_{0\mathbf{k} + \mathbf{q}, l'} - \epsilon_{0\mathbf{k}, l} + \hbar\omega + is} \langle \mathbf{k}, l | V | \mathbf{k} + \mathbf{q}, l' \rangle. \end{aligned} \quad (13)$$

The indices  $l$  and  $l'$  range over all the bands in bismuth. We now wish to show that we need retain only those matrix elements of  $\rho_1$  for which (a)  $l = l'$  ( $l'$  is only the hole or conduction band), and (b)  $\mathbf{k}$  and  $\mathbf{k} + \mathbf{q}$  are both in the neighborhood of the same band extremum.

Assuming that  $V(\mathbf{x})$  is sufficiently smooth, and of long-range character, the matrix element in the right-hand side of Eq. (13) may be approximated:

$$\begin{aligned} \langle \mathbf{k}, l | V | \mathbf{k} + \mathbf{q}, l' \rangle &= \int u_{\mathbf{k}, l}^\dagger u_{\mathbf{k} + \mathbf{q}, l'} e^{i\mathbf{q} \cdot \mathbf{x}} V(\mathbf{x}) d\mathbf{x} \\ &\approx (\mathbf{k}, l | \mathbf{k} + \mathbf{q}, l') V_{\mathbf{q}}, \end{aligned} \quad (14)$$

where

$$(\mathbf{k}, l | \mathbf{k} + \mathbf{q}, l') \equiv v_a^{-1} \int_c u_{\mathbf{k}, l}^\dagger u_{\mathbf{k} + \mathbf{q}, l'} d\mathbf{x}, \quad (15)$$

$v_a$  is the unit cell volume,  $c$  is a unit cell, and where we have expanded  $V(\mathbf{x})$  by

$$V(\mathbf{x}) = \sum_{\mathbf{q}} e^{-i\mathbf{q} \cdot \mathbf{x}} V_{\mathbf{q}}. \quad (16)$$

The summation in Eq. (16) extends over all  $\mathbf{q}$  space; the approximation of Eq. (14) assumes  $V_{\mathbf{q}}$  is negligible when  $\mathbf{q}$  is outside the zone. For an ionized impurity in the isotropic electron gas,  $V_{\mathbf{q}}$  approaches a nonzero limit as  $q \rightarrow 0$ , and goes as  $q^{-2}$  for large  $q$ . We assume, and indeed will find, this behavior in bismuth.

Referring to Eq. (13), and setting  $\omega = 0$  for a static impurity potential, we first suppose  $l \neq l'$ . Then we assume that either (a)  $q$  is sufficiently large that  $V_{\mathbf{q}}$  is negligibly small, or (b) if  $q$  is small, then the bands are well separated and the large energy denominator makes the right-hand side of Eq. (13) negligibly small. The exception to (b) occurs if either  $\mathbf{k}$  or  $\mathbf{k} + \mathbf{q}$  is in the elec-

tron band while the other is the valence band, and both vectors lie near the band extremum  $\mathbf{k}_0$ . In this case,

$$(\mathbf{k}, l | \mathbf{k} + \mathbf{q}, l') \approx (\mathbf{k}_0, l | \mathbf{k}_0, l') = 0, \quad (17)$$

since the band-edge wave functions are orthogonal.

Now, if  $l = l'$  is any band other than the hole or conduction band, the band is either full or empty, in which case Eq. (13) is identically zero.

If, say,  $l = l'$  is the conduction band, then one of the vectors  $\mathbf{k}$  and  $\mathbf{k} + \mathbf{q}$  must be inside an electron ellipsoid and the other outside the ellipsoid for nonzero matrix element of  $\rho_1$ . Suppose  $\mathbf{k}$  lies inside ellipsoid  $i$ . Since  $V_{\mathbf{q}}$  falls off rapidly, and since the energy denominator increases for large  $q$ , we introduce little error if we use the energy-versus-momentum relation (2) over all  $\mathbf{k}$  space ( $\mathbf{k}$  being measured from the band minimum of ellipsoid  $i$ ). A similar argument applies for  $\mathbf{k} + \mathbf{q}$  inside the ellipsoid and for the hole ellipsoid.

These arguments show that the only sizable matrix elements of  $\rho_1$  are those where  $\mathbf{k}$  and  $\mathbf{k} + \mathbf{q}$  are in the same band and are in the neighborhood of the same band extremum; moreover, they show that the matrix elements may be evaluated assuming the validity of Eqs. (2) and (4) over all  $\mathbf{k}$  space. Thus we may reduce  $\rho_1$  to four independent density matrices  $\rho_{1A}$ ,  $\rho_{1B}$ ,  $\rho_{1C}$ , and  $\rho_{1H}$ , the first three applying to the three electron ellipsoids and the fourth to the hole ellipsoid. Utilizing these results, we have, setting  $\omega = 0$ ,

$$\langle \mathbf{k} | \rho_{1i} | \mathbf{k} + \mathbf{q} \rangle = \frac{f_0(\epsilon_{0\mathbf{k} + \mathbf{q}, i}) - f_0(\epsilon_{0\mathbf{k}, i})}{\epsilon_{0\mathbf{k} + \mathbf{q}, i} - \epsilon_{0\mathbf{k}, i} + is} V_{\mathbf{q}}, \quad (18)$$

where  $\mathbf{k}$  and  $\mathbf{k} + \mathbf{q}$  have the same spin; otherwise the matrix element vanishes.

Our final step is one where we look at the details of the potential  $V(\mathbf{x})$ . We take the point of view in which the potential  $V(\mathbf{x})$  consists of a "bare" potential  $V_0$  plus a screening potential  $V_s$ , so that

$$V_{\mathbf{q}} = V_{0\mathbf{q}} + V_{s\mathbf{q}}. \quad (19)$$

The induced electron density  $n_1$  is

$$n_1 = \sum_{\mathbf{q}} e^{-i\mathbf{q} \cdot \mathbf{x}} \sum_{\mathbf{k}, i} \langle \mathbf{k} | \rho_{1i} | \mathbf{k} + \mathbf{q} \rangle \equiv \sum_{\mathbf{q}} e^{-i\mathbf{q} \cdot \mathbf{x}} n_{1\mathbf{q}}, \quad (20)$$

and  $V_s$  and  $n_1$  are related by the Maxwell equation

$$\nabla \cdot \boldsymbol{\epsilon}_l \cdot [-\nabla(V_s / -e)] = -4\pi e n_1. \quad (21)$$

Thus,

$$\mathbf{q} \cdot \boldsymbol{\epsilon}_l \cdot \mathbf{q} V_{s\mathbf{q}} = 4\pi e^2 n_{1\mathbf{q}}, \quad (22)$$

so that

$$\begin{aligned} \langle \mathbf{k} | \rho_{1i} | \mathbf{k} + \mathbf{q} \rangle &= \frac{f_0(\epsilon_{0\mathbf{k} + \mathbf{q}, i}) - f_0(\epsilon_{0\mathbf{k}, i})}{\epsilon_{0\mathbf{k} + \mathbf{q}, i} - \epsilon_{0\mathbf{k}, i} + is} \\ &\quad \times (V_{0\mathbf{q}} + (4\pi e^2 / \mathbf{q} \cdot \boldsymbol{\epsilon}_l \cdot \mathbf{q}) n_{1\mathbf{q}}). \end{aligned} \quad (23)$$

Substituting (20) for the left-hand side of (23) (after

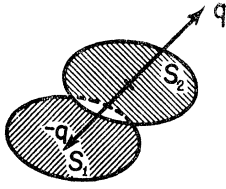


FIG. 3. Volumes in  $\mathbf{k}$  space for summations in  $R_{i\mathbf{q}}$ .

summing over  $\mathbf{k}, i$ ), we have

$$n_{1\mathbf{q}} = \sum_{\mathbf{k}, i} \frac{f_0(\epsilon_{0\mathbf{k}+\mathbf{q},i}) - f_0(\epsilon_{0\mathbf{k},i})}{\epsilon_{0\mathbf{k}+\mathbf{q},i} - \epsilon_{0\mathbf{k},i} + i\delta} \times (V_{0\mathbf{q}} + (4\pi e^2/\mathbf{q} \cdot \boldsymbol{\epsilon}_l \cdot \mathbf{q})n_{1\mathbf{q}}), \quad (24)$$

and hence

$$n_{1\mathbf{q}} = \frac{V_{0\mathbf{q}} \sum_i R_{i\mathbf{q}}}{1 - (4\pi e^2/\mathbf{q} \cdot \boldsymbol{\epsilon}_l \cdot \mathbf{q}) \sum_i R_{i\mathbf{q}}}, \quad (25)$$

where

$$R_{i\mathbf{q}} \equiv \sum_{\mathbf{k}} \frac{f_0(\epsilon_{0\mathbf{k}+\mathbf{q},i}) - f_0(\epsilon_{0\mathbf{k},i})}{\epsilon_{0\mathbf{k}+\mathbf{q},i} - \epsilon_{0\mathbf{k},i} + i\delta}. \quad (26)$$

Using Eq. (22), we have

$$V_{s\mathbf{q}} = (4\pi e^2/\mathbf{q} \cdot \boldsymbol{\epsilon}_l \cdot \mathbf{q})n_{1\mathbf{q}}, \quad (27)$$

so that the perturbation potential matrix element is

$$V_{\mathbf{q}} = \frac{V_{0\mathbf{q}}}{1 - (4\pi e^2/\mathbf{q} \cdot \boldsymbol{\epsilon}_l \cdot \mathbf{q}) \sum_i R_{i\mathbf{q}}}. \quad (28)$$

Equation (28) will be used in a subsequent paper<sup>5</sup> for calculating Alfvén-wave relaxation times in bismuth.

### III. INDUCED ELECTRON DENSITY NEAR AN IONIZED IMPURITY

To calculate  $n_{i\mathbf{q}}$  or  $V_{\mathbf{q}}$  we must evaluate the sums  $R_{i\mathbf{q}}$ . Treating electron ellipsoid  $i$  first, we observe that we get nonzero contributions to the sum  $R_{i\mathbf{q}}$  from only those vectors  $\mathbf{k}$  (now measured from the band minimum) and  $\mathbf{q}$  such that either  $\mathbf{k}$  is inside ellipsoid  $i$  and  $\mathbf{k}+\mathbf{q}$  outside, or vice versa. We can then separate  $R_{i\mathbf{q}}$ :

$$R_{i\mathbf{q}} = \sum_{\mathbf{k} \in S_1} \frac{2}{\epsilon_{0\mathbf{k}+\mathbf{q},i} - \epsilon_{0\mathbf{k},i} + i\delta} + \sum_{\mathbf{k} \in S_2} \frac{-2}{\epsilon_{0\mathbf{k}+\mathbf{q},i} - \epsilon_{0\mathbf{k},i} + i\delta}, \quad (29)$$

where  $\mathbf{k}$  does not include spin, the factor of 2 taking Kramers degeneracy into account, and where the regions  $S_1$  and  $S_2$  for a typical  $\mathbf{q}$  are shown in Fig. 3. As in the case of the isotropic electron gas, it can be shown that the imaginary part of  $R_{i\mathbf{q}}$  is zero, that the two sums in Eq. (29) are equal and that the range of  $\mathbf{k}$  in the second sum may be extended over the entire ellipsoid  $i$  without altering the result. Thus,

$$R_{i\mathbf{q}} = -4 \sum_{\mathbf{k} \in i} \frac{1}{\epsilon_{0\mathbf{k}+\mathbf{q},i} - \epsilon_{0\mathbf{k},i}} = -\frac{1}{2\pi^3} \int_i d\mathbf{k} \frac{1}{\epsilon_{0\mathbf{k}+\mathbf{q},i} - \epsilon_{0\mathbf{k},i}}. \quad (30)$$

The electron energy is given by Eq. (2). Inserting this expression into Eq. (30), we obtain

$$R_{i\mathbf{q}} = -\frac{1}{\pi^3 \epsilon_G} \int_i d\mathbf{k} \frac{1}{[1 + (2\hbar^2/\epsilon_G)(\mathbf{k}+\mathbf{q}) \cdot \boldsymbol{\alpha}^{(i)} \cdot (\mathbf{k}+\mathbf{q})]^{1/2} - [1 + (2\hbar^2/\epsilon_G)\mathbf{k} \cdot \boldsymbol{\alpha}^{(i)} \cdot \mathbf{k}]^{1/2}}. \quad (31)$$

Now we make a coordinate transformation into the principal axis system of  $\boldsymbol{\alpha}^{(i)}$ , letting

$$K_j \equiv \hbar k_j [2\alpha_{jj}^{(i)}/\epsilon_G]^{1/2} \quad (32)$$

and

$$Q_j \equiv \hbar q_j [2\alpha_{jj}^{(i)}/\epsilon_G]^{1/2}. \quad (33)$$

This means

$$d\mathbf{k} = \hbar^{-3} [\epsilon_G^3/8 |\boldsymbol{\alpha}^{(E)}|]^{1/2}, \quad (34)$$

where

$$|\boldsymbol{\alpha}^{(E)}| \equiv |\boldsymbol{\alpha}^{(A)}| = |\boldsymbol{\alpha}^{(B)}| = |\boldsymbol{\alpha}^{(C)}|. \quad (35)$$

Then  $R_{i\mathbf{q}}$  becomes

$$R_{i\mathbf{q}} = -\frac{1}{2\pi^3 \hbar^3 \epsilon_G} [\epsilon_G^3/2 |\boldsymbol{\alpha}^{(E)}|]^{1/2} \times \int_{S_1'} \frac{d\mathbf{K}}{[1 + (\mathbf{K}+\mathbf{Q})^2]^{1/2} - [1 + \mathbf{K}^2]^{1/2}}, \quad (36)$$

where the volume  $S_1'$  in  $\mathbf{K}$  space is a sphere of radius

$$K_F = 2[(\epsilon_F/\epsilon_G)(1 + \epsilon_F/\epsilon_G)]^{1/2}. \quad (37)$$

Using spherical coordinates with polar axis along  $\mathbf{Q}$ , after carrying out the angular integration in Eq. (36) we have

$$R_{i\mathbf{q}} = -(1/\pi^2 \hbar^3) [\epsilon_G/2 |\boldsymbol{\alpha}^{(E)}|]^{1/2} I(Q), \quad (38)$$

where  $Q \equiv |\mathbf{Q}|$ , and

$$I(Q) \equiv Q^{-1} \int_0^{K_F} K dK \{ [1 + (K+Q)^2]^{1/2} - [1 + (K-Q)^2]^{1/2} + (1+K^2) \ln [ [1 + (K+Q)^2]^{1/2} - [1 + K^2]^{1/2} ] - (1+K^2) \ln [ [1 + (K-Q)^2]^{1/2} - [1 + K^2]^{1/2} ] \}. \quad (39)$$

For the hole ellipsoid,  $R_{H\mathbf{q}}$  has the form of Eq. (29).

Since the imaginary part of  $R_{Hq}$  is zero, we may go from the "electron" picture of the hole band to the "hole" picture and use Eq. (30) with the expression of Eq. (4) for the energy. Thus,

$$R_{Hq} = -\frac{1}{2\pi^3} \int_{S_2} \frac{d\mathbf{k}}{(\hbar^2/2)(\mathbf{k}+\mathbf{q}) \cdot \boldsymbol{\alpha}^{(H)} \cdot (\mathbf{k}+\mathbf{q}) - (\hbar^2/2)\mathbf{k} \cdot \boldsymbol{\alpha}^{(H)} \cdot \mathbf{k}} \quad (40)$$

In the principal axis system of  $\boldsymbol{\alpha}^{(H)}$ , we define

$$K_j' \equiv \hbar[\frac{1}{2}\alpha_{jj}^{(H)}]^{1/2}k_j, \quad (41)$$

$$Q_j' \equiv \hbar[\frac{1}{2}\alpha_{jj}^{(H)}]^{1/2}q_j, \quad (42)$$

which gives

$$R_{Hq} = -\frac{1}{\pi^3\hbar^3} (2/|\boldsymbol{\alpha}^{(H)}|)^{1/2} \int_{S_2'} \frac{d\mathbf{K}'}{(\mathbf{K}'+\mathbf{Q}')^2 - \mathbf{K}'^2}, \quad (43)$$

where  $S_2'$  is the entire sphere into which the hole ellipsoid has been transformed. This expression is proportional to the familiar Lindhard result:

$$R_{Hq} = -(1/2\pi^2\hbar^3)(2/|\boldsymbol{\alpha}^{(H)}|)^{1/2}J(Q'/K_F'), \quad (44)$$

where

$$J(y) = 1 + (1/y)(1 - y^2/4) \ln |(y+2)/(y-2)| \quad (45)$$

and

$$K_F' = \epsilon_H^{1/2}. \quad (46)$$

The function  $J$  is independent of the band structure of the ellipsoid band to which it applies, whereas expression (39) for  $I$  contains the parameter  $K_F$ . The reason for this is that the expression (2) for the energy of the nonparabolic band contains an extra parameter  $\epsilon_G$ . The function  $I(Q)$  has a singularity at  $Q=2K_F$ , just as  $J(y)$  has a singularity at  $y=2$ . Equation (39) for  $I$  can be integrated analytically; the result is lengthy and will not be quoted here. The asymptotic expressions for  $I$  and  $J$  for large arguments are given in the Appendix. A plot of  $I(Q)$  for  $K_F=4.498$  (using the SBR parameters) is shown in Fig. 4, with a plot of  $J(y)$  for comparison. Alternatively, the expression (39) can be integrated numerically to obtain  $I$  if one chooses to do so. If  $Q < 2K_F$ , the singularity in the integrand at  $K=Q/2$  must be avoided and an approximate analytical integration done over the singularity.

For computational purposes, we used the analytic expression (45) for  $J(y)$  in the region  $0 < y \leq 16$ , and the asymptotic expansion (A2) for  $y > 16$ . The analytic expression for  $I(Q)$  was used for  $0 < Q \leq 11$ , a numerical integration of Eq. (39) for  $11 < Q \leq 57$ , and the asymptotic expansion (A1) for  $Q > 57$ .

The induced electron density around an ionized impurity of charge  $Ze$  is given by the Fourier transform of Eq. (25), using

$$V_{0q} = -4\pi Ze^2/\mathbf{q} \cdot \boldsymbol{\epsilon}_l \cdot \mathbf{q}. \quad (47)$$

The integration was carried out in a dimensionless  $\mathbf{P}$

space with

$$\mathbf{P} \equiv \hbar\mathbf{k}(2m_0\epsilon_G)^{-1/2}, \quad (48)$$

where  $m_0$  is the free-electron mass. Using dimensionless configuration space units

$$\mathbf{R} \equiv (2m_0\epsilon_G)^{1/2}\mathbf{x}/\hbar, \quad (49)$$

we have

$$n_1(\mathbf{R}) = Z(8\pi^3)^{-1} \int d\mathbf{P} e^{i\mathbf{P} \cdot \mathbf{R}} \frac{F_I \sum I(Q_i) + F_J J(Q_H)}{P^2 + F_I \sum I(Q_i) + F_J J(Q_H)}, \quad (50)$$

where the summations are over  $i=A, B, C$ , where

$$F_I = (2/|\boldsymbol{\alpha}^{(B)}| \epsilon_G)^{1/2} (e^2/\pi\hbar\epsilon_l m_0), \quad (51)$$

$$F_J = (2\epsilon_H/|\boldsymbol{\alpha}^{(H)}|)^{1/2} (e^2/\pi\hbar\epsilon_l m_0 \epsilon_G), \quad (52)$$

$$Q_i = [4m_0\mathbf{P} \cdot \boldsymbol{\alpha}^{(i)} \cdot \mathbf{P}]^{1/2} \quad (53)$$

and

$$Q_H = [m_0(\epsilon_G/\epsilon_H)\mathbf{P} \cdot \boldsymbol{\alpha}^{(H)} \cdot \mathbf{P}]^{1/2}. \quad (54)$$

The units of  $n_1$  in Eq. (50) are  $\hbar^{-3}(2m_0\epsilon_G)^{3/2}$ . Here we have assumed that  $\boldsymbol{\epsilon}_l$  is isotropic.

Equation (50) for  $n_1$  must be evaluated by a three-dimensional numerical integration. We have done this

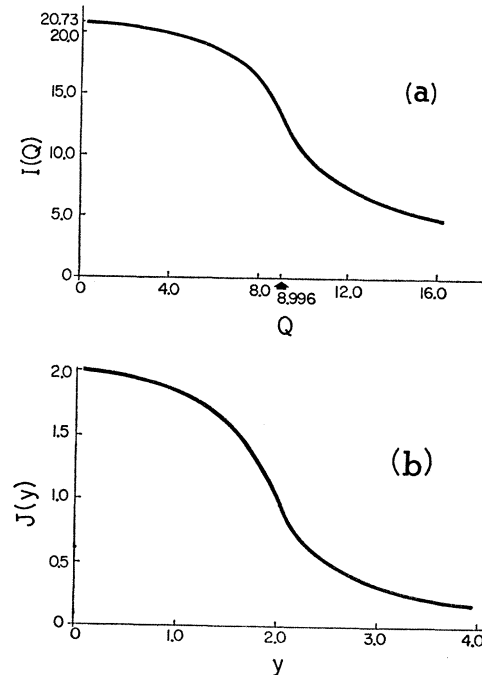


FIG. 4. (a) Plot of  $I(Q)$  for  $K_F=4.498$ , and (b) plot of  $J(y)$ .

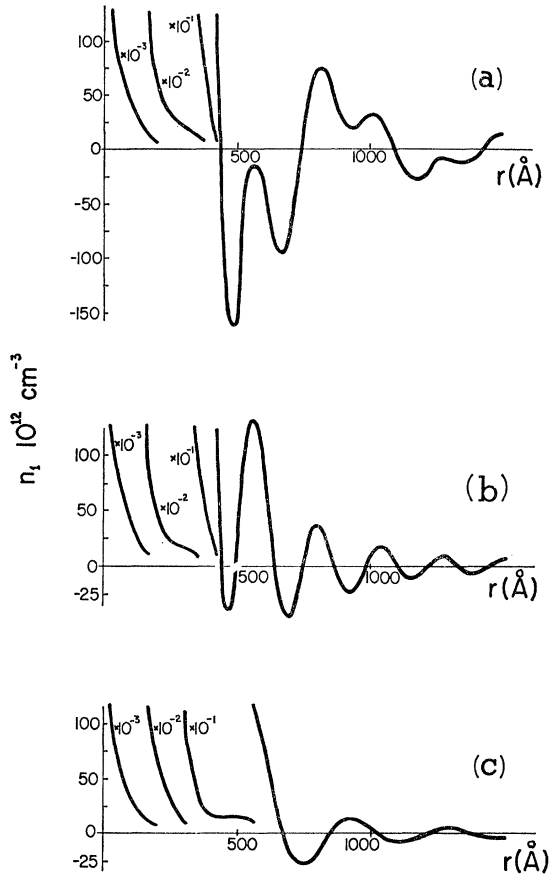


FIG. 5. Plot of  $n_1(r)$  for (a)  $r||$ binary, (b)  $r||$ bisectrix, and (c)  $r||$ trigonal.

for a charge  $Z=1$  for  $\mathbf{R}$  along the binary, bisectrix, and trigonal directions; the results are shown in Fig. 5 and Table II. The units of  $n_1$  here are  $10^{12}$  electrons  $\text{cm}^{-3}$ , and the units of distance in  $\text{\AA}$ .

The integration in Eq. (50) was carried out in cylindrical coordinates with polar axis  $P_z$  parallel to  $\mathbf{R}$ . Defining

$$P_t = (P_x^2 + P_y^2)^{1/2}, \quad (55)$$

then, with  $\varphi$  the azimuthal angle,

$$d\mathbf{P} = P_t dP_t d\varphi dP_z. \quad (56)$$

The integration over  $P_t$  was carried out using the transformation

$$P_t = w/(1-w)^2, \quad 0 \leq w < 1. \quad (57)$$

The integration over  $P_z$  was performed using Filon's rule. We estimate the accuracy of the values in Table II to be  $\pm 10^{12}$  electrons  $\text{cm}^{-3}$ .

#### IV. DISCUSSION OF RESULTS

At large values of  $Q$ ,  $I(Q)$  goes as  $Q^{-1}$ . This behavior results in a logarithmic divergence of  $n_1(\mathbf{R})$  as  $R \rightarrow 0$ ; for parabolic electrons,  $n_1(0)$  is finite. This result for

TABLE II. Values of  $n_1(\mathbf{r})$ , with  $\mathbf{r}$  along the principal crystal axes, for  $Z=1$ . Units of  $n_1$  are  $10^{12} \text{ cm}^{-3}$ .

$r$ ( $\text{\AA}$ )	$n_1$ ( $r  $ bin)	$n_1$ ( $r  $ bis)	$n_1$ ( $r  $ trig)	$r$ ( $\text{\AA}$ )	$n_1$ ( $r  $ bin)	$n_1$ ( $r  $ bis)	$n_1$ ( $r  $ trig)
20	127 800	126 900	117 300	760	30	17	-25
40	98 490	97 350	80 540	780	57	32	-21
60	75 390	74 020	56 270	800	72	38	-15
80	56 550	55 030	40 530	820	74	34	-7
100	41 290	39 720	29 820	840	65	21	0
120	29 270	27 710	22 050	860	51	4	7
140	20 140	18 620	16 310	880	36	-11	12
160	13 510	12 070	12 080	900	25	-21	14
180	8939	7610	8907	920	19	-24	14
200	5979	4781	6487	940	19	-20	13
220	4194	3137	4667	960	23	-12	11
240	3188	2279	3313	980	28	-1	8
260	2640	1878	2302	1000	32	9	4
280	2308	1690	1560	1020	32	15	1
300	2034	1550	1037	1040	28	17	-3
320	1736	1375	676	1060	19	14	-5
340	1390	1140	433	1080	6	7	-7
360	1014	860	283	1100	-7	-1	-8
380	646	572	201	1120	-18	-8	-9
400	323	315	160	1140	-26	-12	-8
420	76	121	146	1160	-29	-12	-6
440	-82	4	147	1180	-28	-9	-3
460	-155	-39	154	1200	-24	-4	-1
480	-163	-26	157	1220	-18	2	1
500	-129	20	156	1240	-12	7	2
520	-80	73	149	1260	-9	10	3
540	-38	115	135	1280	-7	10	4
560	-15	132	116	1300	-8	7	5
580	-15	121	95	1320	-10	3	4
600	-33	88	73	1340	-12	-2	3
620	-60	45	49	1360	-13	-6	2
640	-85	2	26	1380	-12	-8	0
660	-98	-29	7	1400	-9	-7	-2
680	-95	-45	-8	1420	-3	-5	-3
700	-75	-43	-19	1440	3	-2	-3
720	-43	-28	-25	1460	8	2	-3
740	-5	-6	-27	1480	12	4	-3

the nonparabolic electron gas is a consequence of the band structure [Eq. (2)] for large values of  $\mathbf{k}$ ; obviously this expression is valid only in the neighborhood of an electron ellipsoid, so the values of  $n_1(\mathbf{R})$  calculated on the basis of the above theory must be in error for sufficiently small  $\mathbf{R}$ . However, the behavior of  $n_1$  beyond a distance of a few lattice constants from the impurity should be fairly well predicted by this theory.

The plot of  $n_1(\mathbf{R}||$ bisectrix) exhibits oscillations with a period of about 250  $\text{\AA}$ . The plot of  $n_1(\mathbf{R}||$ binary) shows these same oscillations, with oscillations of somewhat larger amplitude and a period of about 700  $\text{\AA}$  superimposed on them. The oscillations in the plot of  $n_1(\mathbf{R}||$ trigonal) are of smaller amplitude, and period about 300  $\text{\AA}$ . These results follow in a simple way from the band structure of bismuth:

It is known<sup>6</sup> that the Friedel oscillations in  $n_1$  for the parabolic isotropic electron gas arise from the singularity in  $J(y)$  at  $y=2$ . The singularity in  $I(Q)$  at  $Q=2K_F$  is of the same type (i.e., the expansions of  $I(Q)$  about  $Q=2K_F$  and  $J(y)$  about  $y=2$  have leading terms of the same form). Furthermore, for large values of  $\mathbf{R}$ , the behavior of  $n_1$  will be dominated by the behavior of the integrand of Eq. (50) in the neighbor-

hood of those points in  $\mathbf{P}$  space, where (a) the integrand has a singularity, and (b), where the phase  $\mathbf{P} \cdot \mathbf{R}$  is stationary for small variations of  $\mathbf{P}$  on the surface where the integrand has the singularity. There are eight such points, two for each carrier ellipsoid. If  $\mathbf{P}_s$  is such a point of stationary phase on a surface of singularity, then  $-\mathbf{P}_s$  is also (by inversion symmetry). In the direction  $\hat{R}$  (unit vector in the direction of  $\mathbf{R}$ ), the behavior of the integrand near  $\mathbf{P}_s$  and  $-\mathbf{P}_s$  will give rise to a term of the form

$$CR^{-3} \cos(R\mathbf{P}_s \cdot \hat{R}), \quad (58)$$

where  $C$  is a constant. One expects that  $C$  will be large when the curvature of the surface  $Q=2K_F$  (or  $y=2$ ) at  $\mathbf{P}_s$  is small, and small when the curvature is large.

In Fig. 5, for  $\mathbf{R}||\text{binary}$ , the long-period, large-amplitude oscillations arise from electron ellipsoid  $A$ . Since

$$\mathbf{P} \cdot \mathbf{R} = \mathbf{k} \cdot \mathbf{r}, \quad (59)$$

and  $\mathbf{P}_s \cdot \hat{R} = 0.151$  in this case, we expect a period  $\Delta r = 657 \text{ \AA}$  for the contribution of ellipsoid  $A$  to  $n_1$  for large  $R$ . For the hole ellipsoid,  $\mathbf{P}_s \cdot \hat{R} = 0.427$ , so it gives rise to oscillations with period  $\Delta r = 232 \text{ \AA}$ .

Electron ellipsoids  $B$  and  $C$  give rise to small-period

oscillations, but the curvature at the appropriate  $\mathbf{P}_s$  is so large that the contributions do not show up in the plot of  $n_1$ .

For  $\mathbf{R}||\text{bisectrix}$ ,  $\mathbf{P}_s \cdot \hat{R}$  and the curvature at  $\mathbf{P}_s$  are the same as in the binary case for the hole ellipsoid, but now for each electron ellipsoid we have large  $\mathbf{P}_s \cdot \hat{R}$  and large curvature, so we see only the hole contribution to  $n_1$  for large  $R$ .

In the case  $\mathbf{R}||\text{trigonal}$ , each electron ellipsoid has  $\mathbf{P}_s \cdot \hat{R} = 0.299$ , with somewhat greater curvature at  $\mathbf{P}_s$  than in the case  $\mathbf{R}||\text{binary}$ .

The hole ellipsoid has  $\mathbf{P}_s \cdot \hat{R} = 1.40$  with large curvature at  $\mathbf{P}_s$ , since  $\mathbf{P}_s$  is the top of the hole ellipsoid. The oscillations in this case are due to the electrons, with somewhat smaller amplitude than in the other two cases, and with period  $\Delta r = 322 \text{ \AA}$ .

#### ACKNOWLEDGMENTS

We wish to thank Dr. George Williams, Rod Isaacson, Peter Temple, Dr. George Gaspari, Dr. M. S. Dresselhaus, and Dr. T. P. Das for many helpful discussions. One of us (D. H. B., Jr.) wishes to thank Dr. Elias Burstein and Dr. Yasuji Sawada for a stimulating discussion.

#### APPENDIX

$$\begin{aligned} I(Q \rightarrow \infty) \approx & (2K_F^3/3)Q^{-1} + \frac{1}{4}\{K_F(1+2K_F^2)(1+K_F^2)^{1/2} - \ln[K_F + (1+K_F^2)^{1/2}]\}Q^{-2} + \{\frac{1}{3}K_F^3 + \frac{2}{5}K_F^5\}Q^{-3} \\ & + \{(8/9)K_F^3(1+K_F^2)^{3/2} - (4/9)K_F(1+K_F^2)^{5/2} + \frac{1}{3}K_F(1+K_F^2)^{3/2} \\ & + \frac{1}{6}K_F(1+K_F^2)^{1/2} + \frac{1}{6}\ln[K_F + (1+K_F^2)^{1/2}]\}Q^{-4} + \{(4/7)K_F^7 + (13/30)K_F^5 - (1/12)K_F^3\}Q^{-5} \\ & + \{(32/15)K_F^5(1+K_F^2)^{3/2} - \frac{2}{3}(K_F^4 + K_F^2 - \frac{3}{8})(1+2K_F^2)K_F(1+K_F^2)^{1/2} \\ & + \frac{1}{8}\ln[1+2K_F^2+2K_F(1+K_F^2)^{1/2}]\}Q^{-6}. \quad (A1) \end{aligned}$$

$$J(y \rightarrow \infty) \approx (8/3)y^{-2} + (32/15)y^{-4} + (128/35)y^{-6}. \quad (A2)$$

$$I(0) = K_F(1+K_F^2)^{1/2}. \quad (A3)$$

$$J(0) = 2. \quad (A4)$$